Molecular Vision 2006; 12:1640-8 <http://www.molvis.org/molvis/v12/a188/>
Received 14 August 2006 | Accepted 21 September 2006 | Published 22 December 2006

Gene expression profile of the adult human retinal ganglion cell layer

Chan Y. Kim,[1,2] Markus H. Kuehn,[1] Abbot F. Clark,[3] Young H. Kwon[1]

[1]Department of Ophthalmology and Visual Sciences, University of Iowa Health Care, 200 Hawkins Drive, Iowa City, IA; [2]Department of Ophthalmology, Institute of Vision Research, Department of Ophthalmology, Yonsei University College of Medicine, Seoul, Korea; [3]Glaucoma Research, Alcon Research Ltd., Fort Worth, TX

Purpose: Pathophysiological events in the retinal ganglion cell layer (GCL) are a prominent feature of several optic neuropathies including glaucoma. The purpose of this study was to identify and catalog genes whose expression in the human retina is restricted to the GCL.

Methods: Laser capture microdissection (LCM) technology was used to isolate tissue from the perimacular retina of three human donors without retinal or optic nerve disease. RNA was isolated from the (1) retinal GCL and (2) the inner and outer nuclear layers of the same retina, and the gene expression profiles of both fractions were determined using Affymetrix Hu133Plus 2.0 GeneChips. Data were analyzed to identify those genes whose expression is substantially more prevalent in the GCL when compared to the outer retinal layers. Differential expression of selected genes was confirmed by real-time PCR and immunohistochemistry.

Results: The results show that mRNA levels of previously described ganglion cell markers, e.g. the neurofilament genes (NEFH, NEF3, or NEFL) and the Brn3a transcription factor (POU4F1), were highly enriched in the isolated GCL fraction. In contrast, transcripts for genes associated with phototransduction (RHO), photoreceptor development (NR2E3), or interphotoreceptor matrix constituents (IMPG1) were nearly absent from the GCL fraction. Using bioinformatics approaches over 80 genes were identified whose expression in the human retina appears to be limited to the GCL.

Conclusions: We have successfully used LCM technology to generate gene expression profiles of highly enriched GCL fractions of the normal human retina. These data not only provide clues to the normal function of retinal ganglion cells but also serve as a resource in the development of ganglion cell specific markers or transfection vectors, and the identification of candidate genes for hereditary forms of glaucoma.

The retinal retinal ganglion cell layer (GCL) is comprised of several distinct cell types located in intimate contact with one another. Most prominent among these are retinal ganglion cells (RGC), astrocytes, and amacrine cells, but microglia are also occasionally observed. In addition, distinct subpopulations of each cell type have been described based on morphological appearance or discrete histochemical markers [1]. To date, information regarding the molecular composition and characteristics of ganglion cell subtypes remains incomplete, particularly with respect to the distinguishing characteristics of individual subtypes of ganglion cells.

The paucity of molecular information about the resident cells of the GCL is partly due to the morphological organization of the tissue where RGC, glial cells, and amacrine cells are found in very close proximity. Amacrine cells in particular represent a sizeable fraction of cells present in this layer, contributing over 50% of cells in the human midperipheral GCL [2]. The identification of gene products that, within the retina, are specific to the GCL, or are highly enriched in the GCL as compared to other retinal layers, would provide useful information for selecting novel molecular markers, identifying functional characteristics of cellular populations, and ultimately aiding in the development of treatment regimens directed at distinct cell types through specific receptors or gene therapy vectors driven by highly selective promoters.

Arguably the most important function of the GCL is the transmission of stimuli from the sensory retina via RGC to the visual centers of the brain. In addition, RGC appear to be involved in other important processes, e.g. melanopsin containing RGC contribute to the regulation of circadian rhythms [3]. A number of ocular neuropathies are accompanied by pathophysiological events in the GCL. Loss of vision in the glaucomas, the most common group of these afflictions, occurs despite adequate photoreceptor function and is caused by the slow, progressive death of RGC [4,5]. While the demise of RGC is ultimately the cause for vision loss, other cell types present in the GCL, in particular microglia or astrocytes, may contribute to this neuronal degeneration through the release of molecules harmful to neurons [6].

Recently several investigators have presented gene expression profiles of rat RGC purified by immunopanning following enzymatic dissociation of the retina [7,8]. This method allows for the isolation of highly enriched RGC fractions. However, it removes the cells from their natural environment and is likely to alter some aspects of the RGC expression profile. One alternative approach is to isolate the cells of the GCL using laser capture microdissection (LCM) and to employ

Correspondence to: Markus Kuehn, Ph.D., Department of Ophthalmology and Visual Sciences, University of Iowa Hospitals and Clinics, Iowa City, IA 52242; Phone: (319) 335-9565; FAX: (319) 353-6641; email: Markus-Kuehn@uiowa.edu

bioinformatics approaches to identify GCL specific gene expression through the computational subtraction of those genes also expressed elsewhere in the retina. While this method is effective to remove genes shared with most cell types, one limitation of this approach is that gene products derived from the astrocytes of the nerve fiber layer can not be reliably excluded. Thus the removal of shared gene transcripts will result in a catalog of genes likely to be either RGC or astrocyte derived. In this report we used LCM to isolate cells from the GCL of three adult normal human eye donors as well as from the inner and outer nuclear and inner and outer plexiform layers from the same donors. The resulting catalog of GCL specific molecules represents a resource for the identification of candidate genes for hereditary forms of glaucoma, bioinformatics analyses of retinal gene expression patterns, and the identification of target molecules for pharmacological approaches aimed at neuroprotection of RGC.

METHODS

Human donor tissue: Human eyes of adult donors without retinal or optic nerve disease (ages 72, 75, and 91) were obtained from the Iowa Lions Eye Bank and preserved within 5 h postmortem (see below). The clinical history of all donors was reviewed by a board certified ophthalmologist (YHK) prior to use of the tissue. Donors included in this study did not have a history of diabetes, age-related macular degeneration, glaucoma, other neurodegenerative diseases, and were without abnormal finding upon dissection (Figure 1).

Laser capture microdissection and RNA isolation: For LCM portions of the neural retina from the central to mid-periphery area were isolated from one eye of the three human donors described above. Tissue was obtained from the area between three disk diameters peripheral to the foveola and the vortex vein inlet (approximately 4.5-10 mm from the foveola). Tissue was embedded in optimal cutting temperature (OCT) medium (Tissue-Tek®, Sakura Finetek, Torrance, CA) without prior fixation and stored at -80 °C until the completion of medical records review.

Tissue was sectioned to a thickness of 7 μm using a cryomicrotome (HM 505E microtome, Microme Laborgeräte, Walldorf, Germany) and dehydrated through a graded series of ethanol followed by incubation in xylenes. Laser capture microdissection was performed using the PixCell® II system (Arcturus Bioscience, Inc., Mountain View, CA) and CapSure® LCM macro caps (Arcturus). Laser settings were from 60 to 100 mW in power, 5.0-10.0 ms in duration, and a laser spot size of 7.5 μm was used. Fractions were captured separately along the entire length of the section and an estimated 1,000 cells were obtained from each sample. Following collection, tissue was removed from the LCM cap and RNA was isolated using the PicoPure® RNA extraction kit (Arcturus) following the manufacturer's protocol, including DNAse treatment, and stored at -80 °C until further processing.

Prior to T7-RNA polymerase based amplification the quality and quantity of the isolated RNA was assessed by real-time PCR. Briefly, 5% of the obtained material was reverse

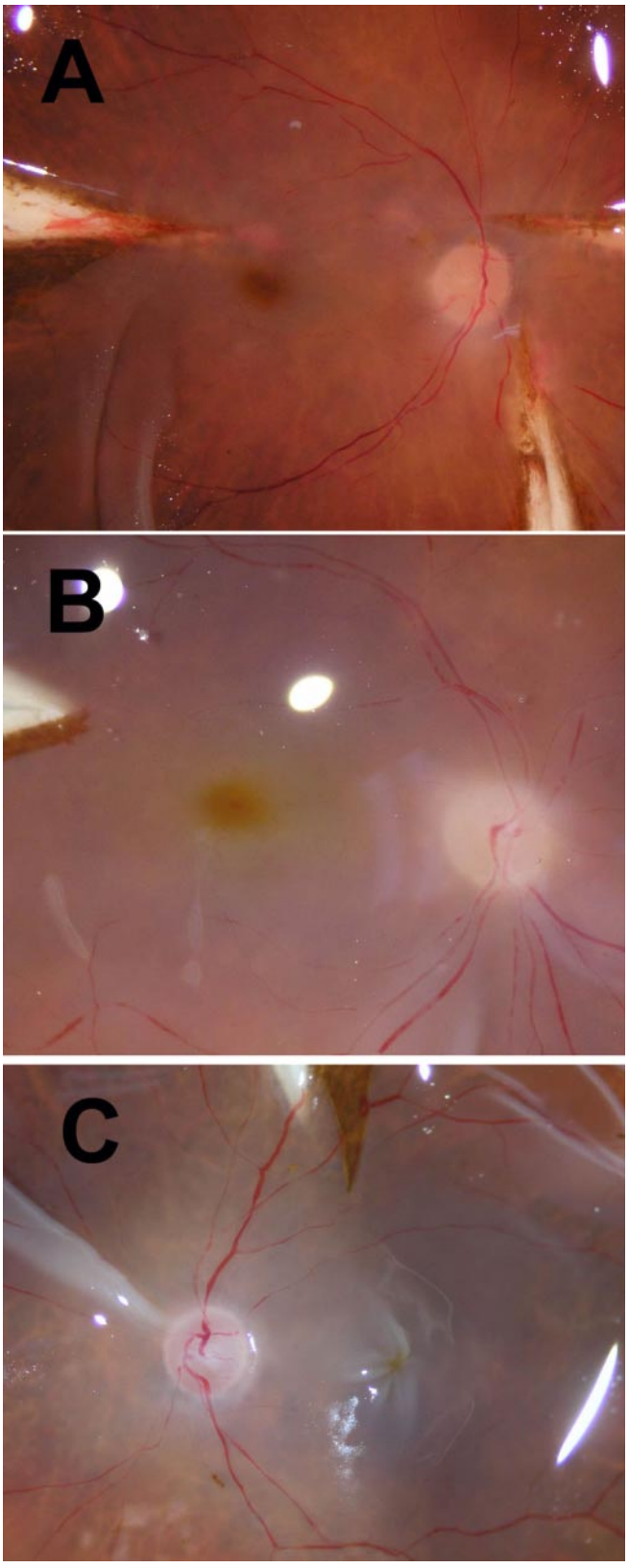

Figure 1. Gross morphological appearance of the human donor eyes used for laser capture microdissection. Only eyes free of ocular pathology based upon donor's chart review and post-mortem retinal examination were used in this study.

transcribed in an oligo(dT)18 primed reaction. Real time PCR was then carried out using the QuantiTect SYBR Green PCR Kit (Qiagen) and an ABI Prism® 7700 Sequence Detection System (Applied Biosystems, Foster City, CA). Amplification values obtained for glyceraldehyde 3-phosphate dehydrogenase (for primer sequences see Table 1) were compared to a standard curve and the approximate yield was calculated.

RNA linear amplification and probe synthesis: Linear amplification and cRNA synthesis were carried out in a two-round amplification protocol using the RiboAmp® HS RNA Amplification Kit (Arcturus). Briefly, 500 pg-1 ng total RNA was reverse transcribed using an oligo(dT) primer bearing a T7 promoter sequence. Following synthesis of double-stranded cDNA, cRNA was created through T7 RNA polymerase based in vitro transcription (IVT). The obtained cRNA was then again converted into cDNA and a second IVT reaction was carried out in the presence of biotinylated UTP and CTP (PerkinElmer, Boston, MA). The resulting biotinylated cRNA was purified and analyzed by agarose gel electrophoresis. Samples displaying adequate size distribution (i.e. majority of product >300 bp) were used directly for gene array analyses.

Array hybridization and data analysis: cRNA probes from each donor's GCL and OR were individually hybridized to Affymetrix Hu133Plus 2.0 GeneChips® (Affymetrix, Inc., Santa Clara, CA) according to the recommendations of the manufacturer (six hybridizations total). The fluorescence signals were detected with an HP GeneArray scanner (Hewlett-Packard, Palo Alto, CA). Data derived were evaluated to ensure that the number of detected genes, the scale factor, and the 5' to 3' probe set values of the housekeeping controls were comparable between all hybridizations. Raw data from all samples were normalized using the GC-RMA algorithm. To ascertain that pure fractions of GCL cells or inner and outer nuclear layer cells were obtained, the detected expression levels of the NR2E3, IMPG1 and NEF3 genes were examined in all samples. These genes are only expressed either in the outer nuclear layer (IMPG1 and NR2E3) or in ganglion cells (NEF3) [9-11]. Only those data sets that displayed at least 50 fold enrichment of these genes in the appropriate fraction were judged to be sufficiently pure to be included in subsequent analysis. The probe sets used were: 207054_at (IMPG1), 208388_at (NR2E3), and 205113_at (NEF3).

Prior to statistical analysis, probe sets that did not display differential expression (i.e. >2 fold expression change between the highest and lowest value) were excluded from further analyses. Likewise, probe sets that did not appear to be expressed in the retina (i.e. normalized expression values >100 in at least one sample) were removed. Expression values were transformed to $\log_2$ based values and statistical significance was calculated by two-tailed paired t-test analysis based upon the data obtained from the GCL and inner and outer nuclear layer fractions of each individual donor. p-values <0.05 were considered significant.

Data were independently analyzed using the Significance Analysis of Microarrays (SAM) algorithm, version 2.21 [12]. A delta value of 0.6 was selected in a two class paired response type analysis. The false discovery rate was estimated through 200 permutation tests, using the K-nearest neighbors as the imputation engine. Under these parameters the false discovery rate was 0% and no false positive signals were predicted when a 10 fold expression change cut-off value was applied.

Real-time PCR: Expression changes were confirmed for selected genes by real-time PCR analysis using the primers listed in Table 1. Independent batches of mRNA were obtained from all donors by LCM as described above. The forward and reverse primers of each primer pair correspond to regions separated by at least one intron to prevent amplification due to trace amounts of genomic DNA. Samples were analyzed in triplicate and PCR reactions were carried out as described above. Expression values were normalized to those of the GAPDH gene as described previously [13].

Immunohistochemistry: Tissue from three additional eye donors was used for immunohistochemistry. Retinal tissue was fixed in 4% paraformaldehyde, infiltrated with increasing concentrations of sucrose and frozen in OCT medium [14]. As above, 7 μm section were cut with a cryo-microtome and incubated with the antibody EH7A (developed by Dr. J.D. Ernst

Table 1. Oligonucleotide primers used during real-time polymerase chain reaction

Gene	Forward Primer (5'-3')	Reverse Primer (5'-3')
PRPH	TAAAGACGACTGTGCCTGAGGT	TCCGGGTCTCAATGGTCTTGAT
STMN2	TGGAGGCTGCAGAGGAAAGAAGAA	TCCGCCATCTTGCTGAAGTTGTTG
SRPX	AGCACAGTGTGGCCTTGATCTT	TAGAGTGGGATTCGCAGCAACA
ELAVL2	TGCTGCCATGGAAACACAACTGTC	TTCCCAGAGTCAACTGGTGACGAA
RBPMS	AACCTCGGGAGCTCTATCTGCTTT	AGCATTCTTTGCAGCCTCTGCT
GAPDH	TGTTGCCATCAATGACCCCTT	CTCCACGACGTACTCAGCG

PRPH represents peripherin; STMA2 represents stathmin-like 2; SRPX represents sushi repeat-containing protein; ELAVL2 represents embryonic lethal, abnormal vision like 2; RBPMS represents RNA-binding protein gene with multiple splicing; GAPDH represents glyceraldehyde-3-phosphate dehydrogenase.

and maintained by the Developmental Studies Hybridoma Bank, University of Iowa) directed against annexins I and II [15]. Antibody binding was visualized using horseradish peroxidase based staining as described previously [13]. Negative controls included sections not exposed to the primary antibody.

RESULTS

Laser capture microdissection (LCM) was used to obtain material from the ganglion cell layer, referred to herein as "GCL fraction" (Figure 2). Care was taken to avoid retinal vessels, although some capillaries could not reliably be identified and may have been inadvertently collected. In addition, a similar amount of material was isolated from both the inner and outer retinal nuclear layers as well as the inner and outer plexiform layers, referred to as the "outer retina" fraction (OR), was obtained and pooled from the same donor eyes. Successful microdissection was initially evaluated through examination of the LCM cap after capture and through examination of the tissue sections before and after LCM (Figure 2). RNA isolated from the collected fractions was amplified and gene expression levels were determined by microarray analyses. The complete data from all six hybridizations are included in Appendix 1.

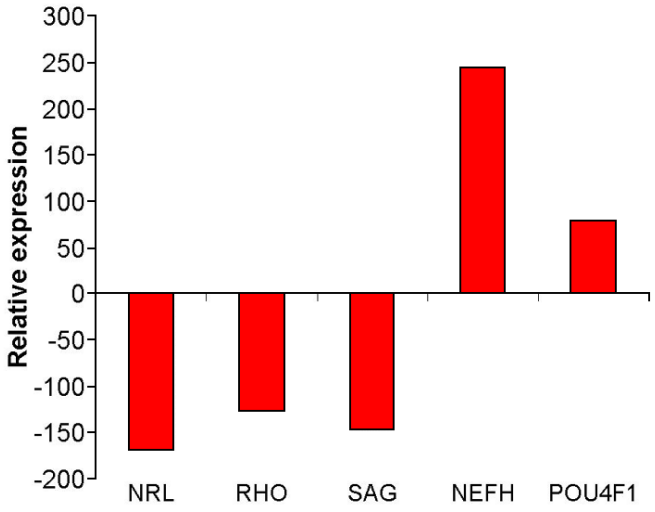

Figure 3. Expression ratios of previously characterized retinal genes. Expression ratios of genes known to be exclusively expressed either in the outer nuclear layer (NRL, SAG, RHO) or the ganglion cell layer (GCL; NFLH, POU4F1) as determined by gene array analysis following laser capture microdissection (LCM). Substantial enrichment of these gene products in the respective fractions indicated successful LCM purification. Relative expression is defined as the ratio between the expression levels detected in the GCL and the OR.

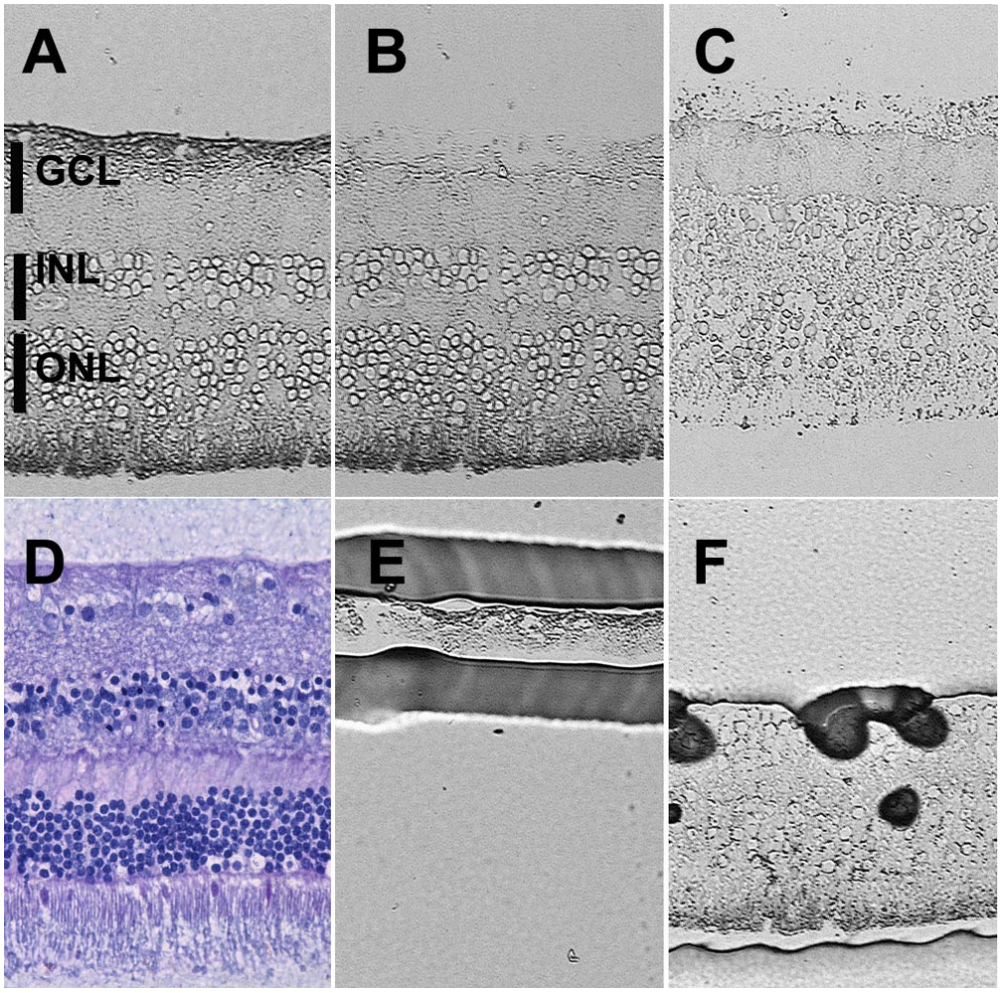

Figure 2. Laser capture microdissection of unfixed sections of human retina. Despite the reduced morphological preservation inherent in unfixed tissue, the distinct layers of the retina are clearly discernible. This series of images demonstrates that isolates of ganglion cell layer (GCL) or OR of high purity can be obtained. **A**: Tissue prior to capture. **B**: Remaining tissue after capture of the GCL, **C**: Remaining tissue after capture of the OR, **E**: isolated GCL material. **F**: Isolated OR material. Vertical bars mark areas collected for analyses. **D**: Histological appearance of adjacent portions of the retina from the same donor stained with hematoxylin and eosin. (INL represents inner nuclear layer, ONL represents outer nuclear layer).

Following microarray analyses the purity of each GCL and OR pair was further evaluated through the comparison of expression values of additional genes that have been previously demonstrated to be selectively expressed either by photoreceptor or ganglion cells. The results demonstrate that relative levels of photoreceptor genes are dramatically reduced in the RGC preparations, whereas gene products that are expressed in RGC are highly enriched and served as further confirmation of sample purity (Figure 3).

Of the over 54,000 probe sets contained on the Genechips used approximately 31% were detected as "present" in each of the GCL samples by the Affymetrix software (GCOS 1.4). We subsequently identified 9,297 probe sets that were consistently present in all GCL samples and sorted them by the average expression level. The resulting list represents a catalog of gene expression in the adult human GCL (Table 2).

Displaced amacrine cells represent a significant portion of all cells in the GCL, but amacrine cells are also present in the inner nuclear layer. Amacrine cell-derived mRNA is expected to be present in both collected fractions, albeit presumably at higher normalized levels in the GCL due to the higher proportion of amacrine cells in the total cell population of the GCL when compared to the inner and outer nuclear cell layers. In order to remove sequences that are likely to be expressed by this cell type, we defined the ratio of expression in the GCL and the OR fraction for the amacrine cell markers parvalbumin, calretinin, and glutamate decarboxylase 1 [16-18]. In our data set we found that these transcripts are 2-4 times more abundant in the GCL fraction than in the OR fraction. Based on these findings, only genes with at least a 10 fold difference between the GCL and OR fractions were further considered. Using Student's t-test, we identified 115 probe sets belonging to 85 different annotated genes that appeared to be significantly enriched in the GCL. Data were also analyzed for differential expression using Significance Analysis of Microarrays (SAM) [12]. Under the condition used, 128 distinct genes were found to be significant which included all but two genes identified by t-test. These identified transcripts most likely represent RGC or retinal astrocyte specific genes (Table 3).

In order to confirm elevated expression in the GCL of a number of the identified genes, we carried out real time PCR analyses for five selected gene transcripts. Preference was given to those genes whose expression pattern in the retina has not been clearly demonstrated, including STMN2 (stathmin-like 2), SRPX (X-linked sushi-repeat-containing protein), ELAV2 (embryonic lethal, abnormal vision-like 2), RBPMS (RNA binding protein with multiple splicing), and PRPH (peripherin, an intermediate neurofilament distinct from the retinal degeneration gene RDS). Data obtained demonstrated that transcripts from these genes are nearly undetectable in the OR but can readily be identified in the GCL fraction (Figure 4).

GCL-specific expression and protein localization of annexin A2 was further evaluated immunohistochemically (Figure 5). Labeling to discrete focal regions in the GCL was reproducibly observed in three individual human donors

Table 2. Transcripts detected at very high levels by gene array analyses of the human ganglion cell layer

Gene Symbol	Title	Avg	Location
TF	Transferrin	34016	Chr:3q21
TUBA3	tubulin, alpha 3	33014	Chr:12q12-12q14.3
NEFH	neurofilament, heavy polypeptide 200kDa	22013	Chr:22q12.2
GABARAPL3	GABA(A) receptors associated protein like 3	20395	Chr:15q26.1
TUBB	tubulin, beta polypeptide	20152	Chr:6p25
GLUL	glutamate-ammonia ligase (glutamine synthase)	20000	Chr:1q31
UBB	ubiquitin B	17999	Chr:17p12-p11.2
NEFL	neurofilament, light polypeptide 68kDa	16727	Chr:8p21
EIF3S6IP	eukaryotic translation initiation factor 3, subunit 6 interacting protein	15487	Chr:22q
PGAM1	phosphoglycerate mutase 1 (brain)	14613	Chr:10q25.3
LDHA	lactate dehydrogenase A	14473	Chr:11p15.4
RTN4	reticulon 4	13537	Chr:2p14-p13
HINT1	histidine triad nucleotide binding protein 1	13491	Chr:5q31.2
LDHB	lactate dehydrogenase B	13217	Chr:12p12.2-p12.1
PGR1	T-cell activation protein	12705	Chr:4p16.1
EEF1A1	eukaryotic translation elongation factor 1 alpha 1	12575	Chr:6q14.1
PTPRO	protein tyrosine phosphatase, receptor type, O	11749	Chr:12p13.3-p13.2
SNAP25	synaptosomal-associated protein, 25kDa	11572	Chr:20p12-p11.2
FTH1	ferritin, heavy polypeptide 1	11147	Chr:11q13
EEF1D	eukaryotic translation elongation factor 1 delta	10951	Chr:8q24.3
SKP1A	S-phase kinase-associated protein 1A (p19A)	10888	Chr:5q31
BEX1	brain expressed, X-linked 1	10679	Chr:Xq21-q23
HSPA8	heat shock 70kDa protein 8	10575	Chr:11q24.1
PCP4	Purkinje cell protein 4	10109	Chr:21q22.2
PARK7	Parkinson disease 7	10079	Chr:1p36.33-p36.12
MAP4	microtubule-associated protein 4	9205	Chr:3p21
ACTG1	actin, gamma 1	9185	Chr:17q25
H3F3A	H3 histone, family 3A	8868	Chr:1q41
COX7A2	cytochrome c oxidase subunit VIIa polypeptide 2	8858	Chr:6q12
RTN1	reticulon 1	8838	Chr:14q21-q22
CALM2	calmodulin 2 (phosphorylase kinase, delta)	8624	Chr:2p21
MAFF	v-maf musculoaponeurotic fibrosarcoma oncogene homolog F (avian)	8476	Chr:22q13.1
INA	internexin neuronal intermediate filament protein, alpha	8327	Chr:10q24.33
PGK1	phosphoglycerate kinase 1	8306	Chr:Xq13
AF1Q	ALL1-fused gene from chromosome 1q	8228	Chr:1q21
YWHAB	tyrosine 3-monooxygenase/tryptophan 5-monooxygenase activation protein, beta polypeptide	8177	Chr:20q13.1
SUI1	putative translation initiation factor	8126	Chr:17q21.31
DDAH1	dimethylarginine dimethylaminohydrolase 1	7979	Chr:1p22
EIF4A2	eukaryotic translation initiation factor 4A, isoform 2	7922	Chr:3q28
MAP1B	microtubule-associated protein 1B	7875	Chr:5q13
NDUFB8	NADH dehydrogenase (ubiquinone) 1 beta subcomplex, 8, 19kDa	7743	Chr:10q23.2-q23.33
K-ALPHA-1	tubulin, alpha, ubiquitous	7606	Chr:12q13.12
STK35	serine/threonine kinase 35	7563	Chr:20p13
NEF3	neurofilament 3 (150kDa medium)	7464	Chr:8p21
TMSB10	thymosin, beta 10	7200	Chr:2p11.2
DRLM	down-regulated in liver malignancy	7138	Chr:4q22.1
MGC14697	upregulated during skeletal muscle growth 5	7091	Chr:10q24.33
FTL	ferritin, light polypeptide	7088	Chr:19q13.3-q13.4
CSRP2	cysteine and glycine-rich protein 2	7075	Chr:12q21.1
SRP14	signal recognition particle 14kDa (homologous Alu RNA binding protein)	6929	Chr:15q22
CYCS	cytochrome c, somatic	6920	Chr:7p15.2
BNIP3	BCL2/adenovirus E1B 19kDa interacting protein 3	6768	Chr:10q26.3
LAMP1	lysosomal-associated membrane protein 1	6631	Chr:13q34
WIF1	WNT inhibitory factor 1	6384	Chr:12q14.1
MDH1	malate dehydrogenase 1, NAD (soluble)	6280	Chr:2p13.3
NARS	asparaginyl-tRNA synthetase	6216	Chr:18q21.2-q21.3
OAZ1	ornithine decarboxylase antizyme 1	6180	Chr:19p13.3
STOM	stomatin	6141	Chr:9q34.1
GNAS	GNAS complex locus	6123	Chr:20q13.2-q13.3
NGFRAP1	nerve growth factor receptor (TNFRSF16) associated protein 1	6121	Chr:Xq22.2
DBI	diazepam binding inhibitor (GABA receptor modulator, acyl-Coenzyme A binding protein)	6069	Chr:2q12-q21
TSC22	transforming growth factor beta-stimulated protein TSC-22	6016	Chr:13q14
ATP6V0E	ATPase, H+ transporting, lysosomal 9kDa, V0 subunit e	5995	Chr:5q35.2
FDFT1	farnesyl-diphosphate farnesyltransferase 1	5981	Chr:8p23.1-p22
SAT	spermidine/spermine N1-acetyltransferase	5950	Chr:Xp22.1
ATP5A1	ATP synthase, H+ transporting, mitochondrial F1 complex, alpha subunit, isoform 1, cardiac muscle	5922	Chr:18q12-q21
MTCH1	mitochondrial carrier homolog 1 (C. elegans)	5785	Chr:6pter-p24.1
HIG1	likely ortholog of mouse hypoxia induced gene 1	5775	Chr:3p21.33
GPX3	glutathione peroxidase 3 (plasma)	5591	Chr:5q23
CFL1	cofilin 1 (non-muscle)	5544	Chr:11q13
MYL6	myosin, light polypeptide 6	5492	Chr:12q13.13
LAPTM4B	lysosomal associated protein transmembrane 4 beta	5487	Chr:8q22.1
NPM1	nucleophosmin (nucleolar phosphoprotein B23)	5380	Chr:5q35
APP	amyloid beta (A4) precursor protein	5376	Chr:21q21.2
CIRBP	cold inducible RNA binding protein	5351	Chr:19p13.3
B2M	beta-2-microglobulin	5308	Chr:15q21-q22.2
DP1	polyposis locus protein 1	5305	Chr:5q22-q23
CDIPT	CDP-diacylglycerol--inositol 3-phosphatidyltransferase	5281	Chr:16p12.1
VAMP1	vesicle-associated membrane protein 1	5207	Chr:12p
SMT3H2	SMT3 suppressor of mif two 3 homolog 2 (yeast)	5154	Chr:17q25
EEF1G	eukaryotic translation elongation factor 1 gamma	5131	Chr:11q12.3
COX5A	cytochrome c oxidase subunit Va	5118	Chr:15q25
SPARCL1	SPARC-like 1 (mast9, hevin)	5077	Chr:4q22.1
UBC	ubiquitin C	5067	Chr:12q24.3
KARS	lysyl-tRNA synthetase	5007	Chr:16q23-q24
C6orf53	chromosome 6 open reading frame 53	4996	Chr:6p24.1
VEGF	vascular endothelial growth factor	4983	Chr:6p12
COX4I1	cytochrome c oxidase subunit IV isoform 1	4798	Chr:16q22-qter
STMN2	stathmin-like 2	4788	Chr:8q21.11-q21.12

Although the signal intensity of different probe sets is not strictly correlated, the genes listed here are likely to represent highly abundant transcripts of the ganglion cell layer. Duplicate genes, genes encoding ribosomal proteins, and uncharacterized transcripts or hypothetical proteins have been removed from this list. Average expression values (Avg) are given in normalized fluorescence units. An unabridged table listing all genes expressed in the GCL is included in Appendix 1.

Table 3. Genes expressed predominately in the ganglion cell layer

Gene Symbol	Title	GCL	OR	Fold change
Transcriptional regulation and RNA binding molecules				
EBF	olfactory neuronal transcription factor 1	638.1	24.2	26.3
EIF5A2	eukaryotic translation initiation factor 5A2	237.4	10.5	22.6
ELAVL2	ELAV (embryonic lethal, abnormal vision)-like 2	476.3	11.3	42.1
ELAVL4	ELAV (embryonic lethal, abnormal vision)-like 4	358.2	24.1	14.8
FKBP1B	FK506 binding protein 1B, 12.6 kDa	1760.7	127.4	13.8
KIAA1045	KIAA1045 protein	224.6	16.7	13.4
POU4F1	POU domain, class 4, transcription factor 1	719.7	9.1	79.1
RBPMS	RNA binding protein with multiple splicing	832.5	12.6	66.0
RBPMS2	RNA-binding protein with multiple splicing 2	172.0	5.5	31.1
TGFB1I1	transforming growth factor beta 1 induced transcript 1	149.3	10.6	14.1
Cytoskeleton/Neurofilaments				
EPPK1	epiplakin 1	175.3	9.4	18.7
KIF5A	kinesin family member 5A	722.9	43.3	16.7
MAP1A	microtubule-associated protein 1A	403.0	37.8	10.7
MICAL2	flavoprotein oxidoreductase, microtubule associated	969.4	51.4	18.9
NEF3	neurofilament 3 (150kDa medium)	6984.1	31.7	220.6
NEFH	neurofilament, heavy polypeptide 200kDa	21899.1	89.4	245.0
NEFL	neurofilament, light polypeptide 68kDa	7843.1	50.5	155.3
PRPH	Peripherin	1238.5	18.4	67.5
TMSB10	thymosin, beta 10	7124.3	324.6	21.9
Endocytosis/neurotransmitter transport/synaptic transmission				
ANXA2	annexin A2	2221.4	37.5	59.3
AP1G1	adaptor-related protein complex 1, gamma 1 subunit	124.4	11.2	11.1
CHRNB3	cholinergic receptor, nicotinic, beta polypeptide 3	134.8	7.6	17.8
CPLX1	complexin 1	380.2	18.2	20.9
GNAS	GNAS complex locus	866.0	75.9	11.4
QPRT	quinolinate phosphoribosyltransferase	178.7	15.2	11.8
RAB13	RAB13, member RAS oncogene family	1802.7	59.7	30.2
STMN2	stathmin-like 2	4139.9	147.9	28.0
STXBP6	syntaxin binding protein 6 (amisyn)	332.8	18.3	18.2
SYNGR3	synaptogyrin 3	981.6	84.3	11.6
Ion/Anion transport				
ATP1B1	ATPase, Na+/K+ transporting, beta 1 polypeptide	3803.3	299.2	12.7
KCNA2	potassium voltage-gated channel, shaker-related subfamily, member 2	302.9	21.5	14.1
KCNJ8	potassium inwardly-rectifying channel, subfamily J, member 8	99.0	8.8	11.3
SCN1A	sodium channel, voltage-gated, type I, alpha	159.3	9.8	16.2
SCN1B	sodium channel, voltage-gated, type I, beta	355.5	17.3	20.5
SCN4B	sodium channel, voltage-gated, type IV, beta	411.7	4.9	84.3
SLC17A6	solute carrier family 17, member 6; VGLUT2	1302.9	10.3	126.8
SLC4A11	solute carrier family 4, sodium bicarbonate transporter-like, member 11	257.4	12.7	20.3
Cell adhesion				
FAT3	FAT tumor suppressor homolog 3 (Drosophila)	662.5	56.7	11.7
FN1	fibronectin 1	221.3	18.5	12.0
GJA1	gap junction protein, alpha 1, 43kDa (connexin 43)	680.4	17.0	40.1
PCDH7	BH-protocadherin (brain-heart)	626.5	50.2	12.5
SRPX	sushi-repeat-containing protein, X-linked	215.5	7.2	30.0
THY1	Thy-1 cell surface antigen	797.8	59.2	13.5
ECM organization				
CTHRC1	collagen triple helix repeat containing 1	201.9	5.9	34.5
LAMA4	laminin, alpha 4	109.9	8.3	13.3
SERPINE2	serine (or cysteine) proteinase inhibitor, clade E member 2	87.3	7.8	11.2
Neuronal development				
CRTAC1	cartilage acidic protein 1	4478.6	347.0	12.9
GAP43	Axonal membrane protein GAP-43	370.5	23.9	15.5
NRG1	neuregulin 1	706.3	24.7	28.6
NRN1	neuritin 1	376.6	12.1	31.1
Fatty acid metabolism				
FABP3	fatty acid binding protein 3, muscle and heart	1054.6	24.9	42.4
LSS	lanosterol synthase	203.0	15.2	13.3
Signal transduction				
GPR54	G protein-coupled receptor 54	322.3	17.2	18.8
RGS1	regulator of G-protein signalling 1	853.7	44.4	19.2
RGS5	regulator of G-protein signalling 5	286.0	24.5	11.7
RIT2	Ras-like without CAAX 2	182.2	7.5	24.2
Apoptosis				
IER3	immediate early response 3	1836.0	144.9	12.7
LGALS1	lectin, galactoside-binding, soluble, 1 (galectin 1)	237.1	12.1	19.6
TNFRSF21	tumor necrosis factor receptor superfamily, member 21	469.0	14.9	31.6
Miscellaneous				
GGH	gamma-glutamyl hydrolase	243.9	22.1	11.1
HBA2	hemoglobin, alpha 2	222.3	6.7	33.0
HHL	expressed in hematopoietic cells, heart, liver	513.2	41.3	12.4
HLA-DPA1	major histocompatibility complex, class II, DP alpha 1	4600.0	126.9	36.3
LMO2	LIM domain only 2 (rhombotin-like 1)	313.5	20.5	15.3
MT3	metallothionein 3 (growth inhibitory factor (neurotrophic))	646.8	57.6	11.2
PECAM1	platelet/endothelial cell adhesion molecule (CD31 antigen)	964.5	83.0	11.6
PPP2R2C	protein phosphatase 2, regulatory subunit B gamma	287.8	26.7	10.8
UCHL1	ubiquitin carboxyl-terminal esterase L1	681.9	33.8	20.1

Genes expressed at least at 10 fold higher levels in the GCL than in other parts of the retina, as identified both by SAM and t-test, and grouped by putative function. Hypothetical gene products or uncharacterized sequences were removed from this list. Average expression values (ganglion cell layer and OR) are given in normalized fluorescence units.

whereas only minor reactivity was observed in other portions of the neural retina. However, large retinal and choroidal vessels also displayed marked immunoreactivity (data not shown). The observed labeling with the annexin antibody did not co-localize with antibodies directed against the cell type markers CD68 (microglia), GFAP (astrocytes), or ThyI (RGC).

DISCUSSION

LCM has been used extensively for analyses at the DNA and RNA level, and numerous studies have described the use of laser-captured material for global analyses of gene expression using cDNA microarrays [19]. The development of various protocols for linear amplification of mRNA facilitated the investigation of small amounts of RNA template and has been shown to maintain relative mRNA levels both when amplified samples are compared to one other as well as when compared to unamplified samples [20,21]. Herein we used both LCM and microarray analyses to determine the expression profile of the human adult retinal GCL and to identify those genes whose expression is limited to this retinal layer.

The microarrays used contain over 54,000 probe sets which likely represent the vast majority of all genes of the human genome. Of these, we detected over 9,200 genes which appear to be consistently present in the human GCL, although it is possible that a small fraction of expressed genes might remain undetected due to poor probe set design, insufficient length of the synthesized cRNA probe, or other technical factors. In addition, while RNA quality from donor eyes preserved within a short time after death is generally high [22], it is conceivable that the absence or presence of individual gene products is influenced by post-mortem events, such as cessation of perfusion.

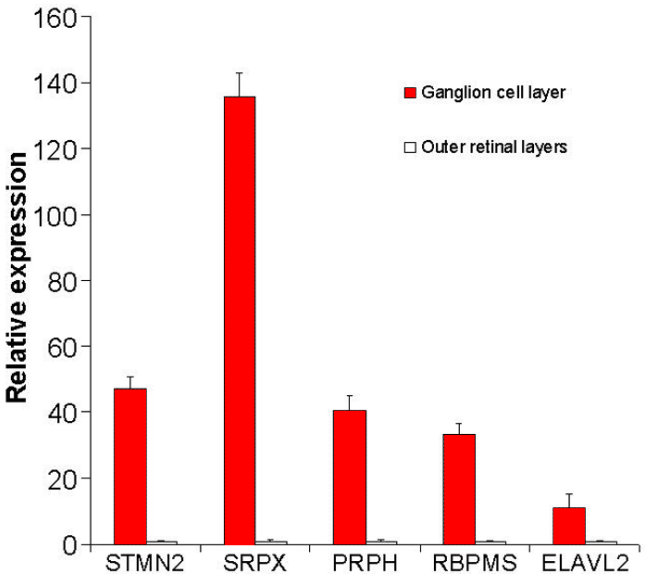

Figure 4. Real-time PCR confirmation of ganglion cell layer specific gene expression. Transcripts for all analyzed genes were either absent or present at very low levels in the OR fraction whereas they were readily detected in the ganglion cell layer.

These genes may be expressed by any of the cell types residing in the GCL: various subtypes of RGC, amacrine cells, glia or endothelial cells and pericytes. Comparison of the genes expressed in the GCL to those expressed in other portions of the retina allowed the identification of over 80 genes whose expression appears to be limited to the GCL. Since RGC and astrocytes are only found in the GCL, it is likely that these cell types contribute the vast majority of the GCL-specific transcripts. However, it is conceivable that GCL-specific transcripts exist in cell types present throughout the retina (e.g. microglia, capillary pericytes or Mueller cell end feet).

Although the functions of many of the identified genes are incompletely described in the literature, we noted several distinct functional groups among the GCL-specific genes. The first group contains genes encoding cytoskeletal components, such as the well characterized RGC-specific neurofilaments, and other molecules implicated in cytoskeletal organization, maintenance of axonal caliber, and axonal transport (e.g. epiplakin 1 or the kinesin family member 5A).

Another prominent functional group appears to be related to endo- and exocytosis as well as intracellular vesicular transport. This group includes such genes as CPLX1 (complexin 1), which promotes neurotransmitter release through interaction with the SNARE complex, and RAB13 which specifically mediates endocytic recycling [23,24]. Collectively these molecules may facilitate neurotransmitter release, reuptake and turnover by RGC and their associated glia.

A third prominent group of GCL-specific molecules contains genes involved in gene transcription and RNA processing, including well known RGC-specific transcription factors such as Brn3a [25], but also genes previously undescribed in the human retina such as the ELAVL2 and ELAVL4 transcripts. These genes encode vertebrate homologues of the drosophila ELAV (Embryonic Lethal, Abnormal Vision) gene family, which has been implicated in functions related to mRNA stability and translatability [26].

Finally, we identified a number of GCL transcripts involved in ion and amino acid transport. This group contains several K+ and Ca+ channels, e.g. Kv 1.2 (KCNA2) or voltage gated sodium channels (SCN1A and B), as well as the Na+/K+ transporting beta-1 ATPase (ATP1B1). Voltage-dependent sodium and potassium channels are crucial for the generation and propagation of action potentials and thus to the function of RGC.

Many of the genes identified in our study have previously been reported to be either RGC- or glial cell-specific in a number of studies focused on individual molecules. For example, Fyk-Kolodziej et al. reported that the distribution of the vesicular glutamate transporter SLC17A6 (VGLUT2) is restricted to ganglion cells [27]. In addition, several of the genes identified as GCL-specific in this study, such as stathmin-like2, have also been reported by other investigators employing high-throughput gene expression profiling approaches [7,8]. Others in contrast, have been previously less well characterized. Examples for such genes include SRPX (sushi-repeat-containing protein), which has previously been suspected to be involved in x-linked retinitis pigmentosa, but does not appear to be expressed in the inner or outer nuclear layer [28], or RBPMS (RNA binding protein with multiple splicing) which has not been previously described in the retina [29].

Two previously published studies examined gene expression in purified rat RGCs [7,8]. Farkas and colleagues used a 2-step panning procedure to isolate RGCs from dissociated retinas of Sprague-Dawley rats, followed by RNA extraction, preparation of a cDNA library, and extensive sequencing of this library [8]. Ivanov and colleagues used a similar 2-step panning procedure to purify RGCs from adult Brown-Norway rats, but profiled gene expression using gene chips [7]. When comparing the results of these two studies with our data, it is important to recognize the advantages and limitations of the techniques used. As discussed previously, the retinal GCL contains other cell types in addition to RGCs, and LCM did

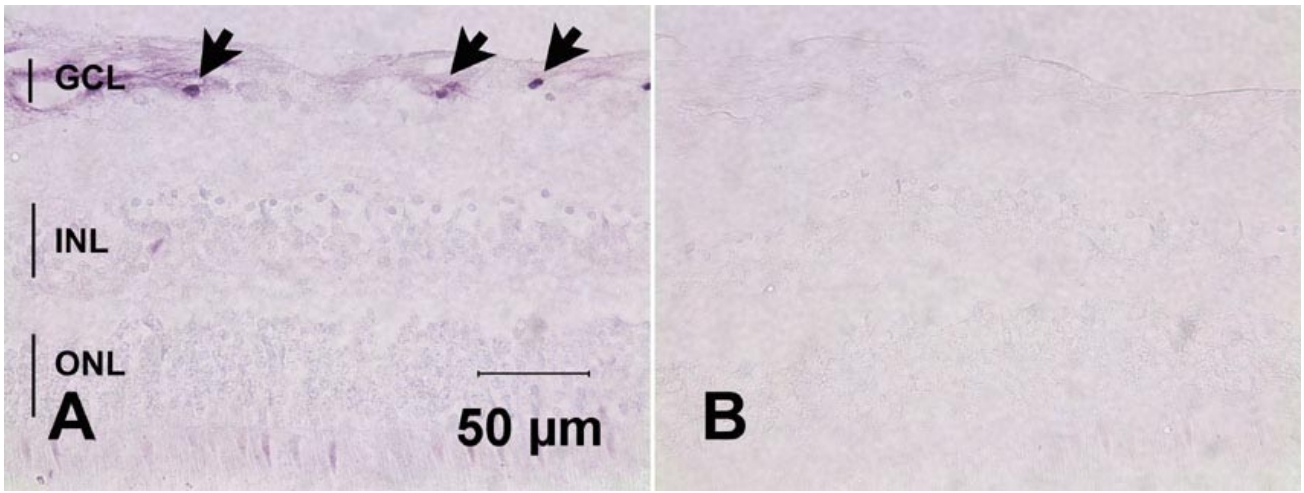

Figure 5. Immunohistochemical detection of annexin II in the normal human retina. In accordance with the observed gene expression profile, annexin immunoreactivity is primarily observed in distinct areas of the GCL (arrows) and, to a lesser degree, diffusely in the nerve fiber layer (**A**). No labeling was observed in the absence of the primary antibody (**B**).

not differentiate between these cell types. In contract, the isolated rat RGC preparations contained >95% RGCs. However, LCM captures the ganglion layer cells in a more natural, native environment. The isolated purified RGCs are axotomized, dissociated from connecting retinal cells, and partially cultured prior to gene expression profiling, which undoubtedly alters the expression of some genes. Despite these important methodological differences between the studies, many of the genes identified in isolated rat RGC could also be detected in this study in the human GCL, including: CHRNB3, PRPH, STMN2, NRN1, NEF3, NEFL, and various members of the RGS family of genes.

The retinal samples evaluated in this study were obtained from near- to mid peripheral portions of the eye. Clearly certain anatomical differences between the ganglion cells of the macula and peripheral retina exist [30]. Accordingly it is likely that the gene expression profile of the macular GCL is in some aspects distinct from the one reported herein. However, the retinal regions evaluated are particularly vulnerable to glaucomatous damage. Despite the wide spread occurrence of glaucoma, relatively little is known about the cellular mechanisms involved in the etiology of the disease or about the genetic risk factors that confer heightened susceptibility to glaucomatous vision loss. The characterization of genes expressed in adult human ganglion or glial cells may be useful in the identification of risk factors or candidate genes for hereditary forms of glaucoma. Furthermore, while apoptosis appears to be the final mechanism of RGC death, other degenerative mechanisms appear to be involved and may be mediated by GCL glial cells [31-34]. Current glaucoma therapy relies upon the reduction of intraocular pressure. Unfortunately, in some patients IOP reduction alone does not completely halt RGC demise and reduction of vision, indicating the need to devise additional treatment regimens aimed specifically at ganglion cell survival. Such approaches might involve the generation of RGC-specific gene therapy vectors or the development of drugs designed to interact specifically with these cells. It is our hope that the data presented will aid in this process.

ACKNOWLEDGEMENTS

This work was supported in part by an unrestricted grant from Research to Prevent Blindness to the UI Department of Ophthalmology.

REFERENCES

1. Masland RH. Neuronal diversity in the retina. Curr Opin Neurobiol 2001; 11:431-6.
2. Curcio CA, Allen KA. Topography of ganglion cells in human retina. J Comp Neurol 1990; 300:5-25.
3. Berson DM, Dunn FA, Takao M. Phototransduction by retinal ganglion cells that set the circadian clock. Science 2002; 295:1070-3.
4. Quigley HA, Broman AT. The number of people with glaucoma worldwide in 2010 and 2020. Br J Ophthalmol 2006; 90:262-7.
5. Van Buskirk EM, Cioffi GA. Glaucomatous optic neuropathy. Am J Ophthalmol 1992; 113:447-52.
6. Kuehn MH, Fingert JH, Kwon YH. Retinal ganglion cell death in glaucoma: mechanisms and neuroprotective strategies. Ophthalmol Clin North Am 2005; 18:383-95,vi.
7. Ivanov D, Dvoriantchikova G, Nathanson L, McKinnon SJ, Shestopalov VI. Microarray analysis of gene expression in adult retinal ganglion cells. FEBS Lett 2006; 580:331-5.
8. Farkas RH, Qian J, Goldberg JL, Quigley HA, Zack DJ. Gene expression profiling of purified rat retinal ganglion cells. Invest Ophthalmol Vis Sci 2004; 45:2503-13.
9. Kobayashi M, Takezawa S, Hara K, Yu RT, Umesono Y, Agata K, Taniwaki M, Yasuda K, Umesono K. Identification of a photoreceptor cell-specific nuclear receptor. Proc Natl Acad Sci U S A 1999; 96:4814-9.
10. Kuehn MH, Hageman GS. Expression and characterization of the IPM 150 gene (IMPG1) product, a novel human photoreceptor cell-associated chondroitin-sulfate proteoglycan. Matrix Biol 1999; 18:509-18.
11. Shaw G, Weber K. The structure and development of the rat retina: an immunofluorescence microscopical study using antibodies specific for intermediate filament proteins. Eur J Cell Biol 1983; 30:219-32.
12. Tusher VG, Tibshirani R, Chu G. Significance analysis of microarrays applied to the ionizing radiation response. Proc Natl Acad Sci U S A 2001; 98:5116-21. Erratum in: Proc Natl Acad Sci U S A 2001; 98:10515.
13. Mullins RF, Skeie JM, Malone EA, Kuehn MH. Macular and peripheral distribution of ICAM-1 in the human choriocapillaris and retina. Mol Vis 2006; 12:224-35.
14. Barthel LK, Raymond PA. Improved method for obtaining 3-microns cryosections for immunocytochemistry. J Histochem Cytochem 1990; 38:1383-8.
15. Ernst JD, Hoye E, Blackwood RA, Mok TL. Identification of a domain that mediates vesicle aggregation reveals functional diversity of annexin repeats. J Biol Chem 1991; 266:6670-3.
16. Kolb H, Zhang L, Dekorver L, Cuenca N. A new look at calretinin-immunoreactive amacrine cell types in the monkey retina. J Comp Neurol 2002; 453:168-84.
17. Casini G, Rickman DW, Trasarti L, Brecha NC. Postnatal development of parvalbumin immunoreactive amacrine cells in the rabbit retina. Brain Res Dev Brain Res 1998; 111:107-17.
18. Famiglietti EV Jr, Vaughn JE. Golgi-impregnated amacrine cells and GABAergic retinal neurons: a comparison of dendritic, immunocytochemical and histochemical stratification in the inner plexiform layer of rat retina. J Comp Neurol 1981; 197:129-39.
19. Gillespie JW, Gannot G, Tangrea MA, Ahram M, Best CJ, Bichsel VE, Petricoin EF, Emmert-Buck MR, Chuaqui RF. Molecular profiling of cancer. Toxicol Pathol 2004; 32:S67-71.
20. Lockhart DJ, Dong H, Byrne MC, Follettie MT, Gallo MV, Chee MS, Mittmann M, Wang C, Kobayashi M, Horton H, Brown EL. Expression monitoring by hybridization to high-density oligonucleotide arrays. Nat Biotechnol 1996; 14:1675-80.
21. Wang E, Miller LD, Ohnmacht GA, Liu ET, Marincola FM. High-fidelity mRNA amplification for gene profiling. Nat Biotechnol 2000; 18:457-9.
22. Malik KJ, Chen CD, Olsen TW. Stability of RNA from the retina and retinal pigment epithelium in a porcine model simulating human eye bank conditions. Invest Ophthalmol Vis Sci 2003; 44:2730-5.
23. Hu K, Carroll J, Rickman C, Davletov B. Action of complexin on SNARE complex. J Biol Chem 2002; 277:41652-6.
24. Morimoto S, Nishimura N, Terai T, Manabe S, Yamamoto Y, Shinahara W, Miyake H, Tashiro S, Shimada M, Sasaki T. Rab13 mediates the continuous endocytic recycling of occludin to the cell surface. J Biol Chem 2005; 280:2220-8. Erratum in: J Biol

Chem 2005; 280:32048.
25. Xiang M, Zhou L, Macke JP, Yoshioka T, Hendry SH, Eddy RL, Shows TB, Nathans J. The Brn-3 family of POU-domain factors: primary structure, binding specificity, and expression in subsets of retinal ganglion cells and somatosensory neurons. J Neurosci 1995; 15:4762-85.
26. Antic D, Lu N, Keene JD. ELAV tumor antigen, Hel-N1, increases translation of neurofilament M mRNA and induces formation of neurites in human teratocarcinoma cells. Genes Dev 1999; 13:449-61.
27. Fyk-Kolodziej B, Dzhagaryan A, Qin P, Pourcho RG. Immunocytochemical localization of three vesicular glutamate transporters in the cat retina. J Comp Neurol 2004; 475:518-30.
28. Meindl A, Carvalho MR, Herrmann K, Lorenz B, Achatz H, Lorenz B, Apfelstedt-Sylla E, Wittwer B, Ross M, Meitinger T. A gene (SRPX) encoding a sushi-repeat-containing protein is deleted in patients with X-linked retinitis pigmentosa. Hum Mol Genet 1995; 4:2339-46.
29. Shimamoto A, Kitao S, Ichikawa K, Suzuki N, Yamabe Y, Imamura O, Tokutake Y, Satoh M, Matsumoto T, Kuromitsu J, Kataoka H, Sugawara K, Sugawara M, Sugimoto M, Goto M, Furuichi Y. A unique human gene that spans over 230 kb in the human chromosome 8p11-12 and codes multiple family proteins sharing RNA-binding motifs. Proc Natl Acad Sci U S A 1996; 93:10913-7.
30. Pavlidis M, Stupp T, Hummeke M, Thanos S. Morphometric examination of human and monkey retinal ganglion cells within the papillomacular area. Retina 2006; 26:445-53.
31. Tezel G, Wax MB. Glial modulation of retinal ganglion cell death in glaucoma. J Glaucoma 2003; 12:63-8.
32. Neufeld AH, Das S, Vora S, Gachie E, Kawai S, Manning PT, Connor JR. A prodrug of a selective inhibitor of inducible nitric oxide synthase is neuroprotective in the rat model of glaucoma. J Glaucoma 2002; 11:221-5.
33. Kuehn MH, Kim CY, Ostojic J, Bellin M, Alward WL, Stone EM, Sakaguchi DS, Grozdanic SD, Kwon YH. Retinal synthesis and deposition of complement components induced by ocular hypertension. Exp Eye Res 2006; 83:620-8.
34. Moreno MC, Campanelli J, Sande P, Sanez DA, Keller Sarmiento MI, Rosenstein RE. Retinal oxidative stress induced by high intraocular pressure. Free Radic Biol Med 2004; 37:803-12.

The appendix is available in the online version of this article at http://www.molvis.org/molvis/v12/a188/.

The print version of this article was created on 22 Dec 2006. This reflects all typographical corrections and errata to the article through that date. Details of any changes may be found in the online version of the article.